mathematics

MDPI

Article

Optimal Propagating Fronts Using Hamilton-Jacobi Equations

Angelo Alessandri [1,*], Patrizia Bagnerini [1], Roberto Cianci [1] and Mauro Gaggero [2]

[1] Department of Mechanical Engineering (DIME), University of Genoa, 16145 Genoa, Italy; bagnerini@dime.unige.it (P.B.); cianci@dime.unige.it (R.C.)
[2] Institute of Marine Engineering (INM), National Research Council of Italy, Via De Marini 6, 16149 Genoa, Italy; mauro.gaggero@cnr.it
* Correspondence: alessandri@dime.unige.it

Received: 7 October 2019; Accepted: 9 November 2019; Published: 16 November 2019

Abstract: The optimal handling of level sets associated to the solution of Hamilton-Jacobi equations such as the normal flow equation is investigated. The goal is to find the normal velocity minimizing a suitable cost functional that accounts for a desired behavior of level sets over time. Sufficient conditions of optimality are derived that require the solution of a system of nonlinear Hamilton-Jacobi equations. Since finding analytic solutions is difficult in general, the use of numerical methods to obtain approximate solutions is addressed by dealing with some case studies in two and three dimensions.

Keywords: Hamilton-Jacobi equation; normal flow equation; level set methods; optimization

1. Introduction

Hamilton-Jacobi equations are well-know partial differential equations (PDEs) that have been successfully used to model moving interfaces. In fact, they are the basis of a widely-studied family of methods usually referred to as level set methods [1]. Hamilton-Jacobi equations are useful not only for the purpose of modeling dynamic fronts, but also to solve optimal control problems over finite and infinite horizons [2], with a number of different applications (see, e.g., [3–5]). In this paper, we propose a novel approach to construct optimal propagating fronts with propagation speed selected in order to minimize a suitable cost functional accounting for a desired front behavior. Sufficient conditions of optimality given by a system of nonlinear Hamilton-Jacobi equations are derived that can be numerically solved when it is difficult to find analytic solutions [6–8].

The propagation of fronts or boundaries separating two regions, either curves in two dimensions or surfaces in three dimensions, is a topic that has gained a lot of attention in the last decades. In fact, modeling the motion of fronts is crucial in different research areas such as, for instance, fluid dynamics and image processing (see, e.g., [9–12] and the references therein). The methods available in the literature for this task are usually catalogued as Lagrangian front tracking and Eulerian front capturing approaches. Front tracking ones are Lagrangian since they rely on the discretization of the front by means of a mesh. A number of points is positioned along the front, and such points are then moved by using ordinary differential equations (ODEs) [13,14]. Lagrangian methods turn out to be quite efficient and precise in applications with fronts characterized by small deformations, but their performances degrade in case of changes of topology, when they need re-meshing upon strong deformations of the boundary. Instead, front capturing methods are Eulerian since the boundary is represented implicitly on fixed grids. Level set methods are an important family of Eulerian approaches that overcome the aforementioned limits of Lagrangian techniques. In such methods, the front is described by the zero level set of a multidimensional function [9]. The possibility to easily account for changes of topology

is one of their main features. The most known methods are those based on the normal flow equation (in which the propagation speed is directed towards the normal to the front) and the mean curvature flow equation (in which the speed is proportional to the curvature of the front in all points). In other words, they differ on the choice of the velocity field in the Hamilton-Jacobi equation.

The literature on the optimal control of infinite-dimensional systems (see [15] for an introduction) is vast and with a special emphasis on fluid flows [16–18], where the problems are addressed in abstract Banach spaces. By contrast, the literature regarding the control of moving fronts is at the very beginning. The control of level sets resulting from a two-phase Stefan problem is investigated in [19,20]. In [21], an original prey-predator model is presented with a predator front modeled as a curve that moves depending on the prey density. More recently, in [22–24], the problem of finding the normal velocity to the front described by level sets of a normal flow equation is attacked with the goal of minimizing a given performance index. After proving the existence of a solution to such a problem, the extended Ritz method is proposed to find suboptimal solutions [7,25]. Such solutions take on the structure of neural networks depending on neural weights, i.e., a set of parameters that need to be tuned. Then, the Gauss-Newton descent method can be used to find an optimal value for the weights, and the resulting algorithm may be viewed as neural learning based on the extended Kalman filter (EKF) [22,24].

As compared with such works, the present paper provides some advances. A new solution paradigm is proposed for the finite-horizon optimal control problem originally proposed in [23,24]. More specifically, sufficient conditions of optimality are rigorously established that require the solution of a system of Hamilton-Jacobi PDEs [26]. Similar conditions are proved for the extension of the same problem to an infinite horizon. Since analytic solutions of such problems are almost impossible to find, approximate solutions are searched for by using a numerical scheme based on the method proposed in [27]. The resulting approach is compared with that of [24,28] both in terms of computational time and ability to optimize the cost functional, thus highlighting the effectiveness of the proposed technique.

The rest of this paper is structured as follows. The main results concerning the considered problems are presented in Section 2. Section 3 describes the numerical results obtained in two case studies. Conclusions and prospect of future work are discussed in Section 4.

The following notation will be adopted throughout the paper. We define $(x, y) := [x^\top, y^\top]^\top$, where $x \in \mathbb{R}^n$ and $y \in \mathbb{R}^m$. Let $\mathcal{X}$ be a real linear normed space of functions with norm $|\cdot|_{\mathcal{X}}$. Given a functional $F : \mathcal{X} \to \mathbb{R}$, F is Fréchet differentiable in $x \in \mathcal{X}$ if there exists a functional $F' : \mathcal{X} \times \mathcal{X} \to \mathbb{R}$ such that

$$F(x + y) = F(x) + F'(x, y) + r(x, y)$$

where $y \in \mathcal{X}$, $F'(x, y)$ is the Fréchet derivative of $F(x)$, and $y \mapsto r(x, y)$ is a remainder of order higher than one, i.e.,

$$\lim_{y \to 0} \frac{r(x, y)}{|y|_{\mathcal{X}}} = 0 .$$

Finally, let $|x| := (x^\top x)^{1/2}$ for any real vector x.

2. Optimal Moving Fronts

In this section, we focus on how moving fronts can be described by level set methods. Toward this end, let $\Omega \subset \mathbb{R}^q$ and $t \in [0, T]$ be a compact space domain of dimension q and $T > 0$ a given time horizon (in the case of infinite horizon problems, we consider the time domain $[0, +\infty)$). A moving front is a curve in two dimensions ($q = 2$) or a surface in three dimensions ($q = 3$) that separates two regions, associated to the zero level set of a function $\phi : \Omega \times [0, T] \to \mathbb{R}$. The boundary $x(t, s)$ is given at time t by the points such that $\phi(x(t, s), t) = 0$, where s is the arc-length parameter of the initial curve $x(0, s)$. Figure 1 displays fronts at time instants t_1 and t_2 together with the corresponding functions ϕ. After differentiating with respect to t, we obtain

$$\phi_t(x,t) + v(x,t) \cdot \nabla\phi(x,t) = 0\,, \tag{1}$$

where $v(x,t) := \frac{d}{dt}x(t,s)$ is the Lagrangian particle velocity representing the direction of propagation of the front at the point $x(t,s)$, and ∇ is the gradient with respect to space. From now on, we refer only to the normal flow equation, in which $v(x,t)$ is chosen proportional to the normal to the front, i.e.,

$$v(x,t) = u\,\frac{\nabla\phi(x,t)}{|\nabla\phi(x,t)|}, \tag{2}$$

where u is the propagation speed. After replacing (2) in (1), we obtain the normal flow equation:

$$\phi_t(x,t) + u\,|\nabla\phi(x,t)| = 0. \tag{3}$$

Equation (3) is associated to initial conditions $\phi_0 : \Omega \to \mathbb{R}$, i.e., $\phi(x,0) = \phi_0(x)$ for all $x \in \Omega$. Usually, ϕ_0 is the signed distance to the initial front. The level set $l \in \mathbb{R}$ of the function ϕ is a set-valued mapping $\Gamma_l : [0,T] \rightrightarrows \mathcal{C}$, where $\Gamma_l(t) := \{x \in \Omega : \phi(x,t) = l\}$.

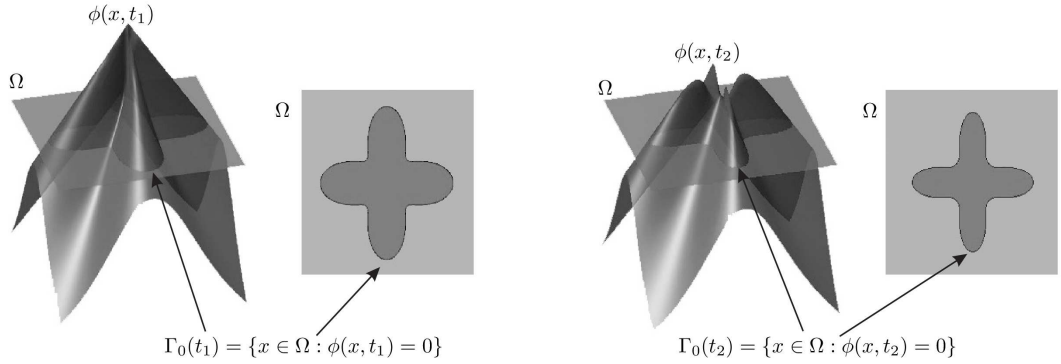

Figure 1. Fronts given by the zero level sets of a multidimensional function ϕ at two different time instants t_1 and t_2.

We deal with the optimal control of (3) via a suitable choice of u. In other words, our aim is to drive the propagating front associated to a certain level set of $\phi(x,t)$ as desired. In practice, the speed function u is considered as a control action depending on time and space, i.e., $u : \Omega \times [0,T] \to \mathbb{R}$. Let us denote by $\mathcal{U}$ the set of admissible control functions, such as the set of measurable bounded functions. This set is made of the smooth functions $(x,t) \mapsto u(x,t)$ such that there exist solutions to the Cauchy problem for (3). Let $\mathcal{F}$ be the space of functions $(t,x) \mapsto \phi(x,t)$ where such a problem is formulated.

The evolution over time and space of a level set of ϕ may be related to a performance indicator depending on the interior or the boundary of the interface (see, e.g., [20]). In this respect, we focus on a cost functional quantifying performances of the control policy, as follows:

$$J(\phi,u) = \int_0^T \int_\Omega h(\phi(x,t),u(x,t),t)\,dx\,dt + \int_\Omega \bar{h}(\phi(x,T))\,dx, \tag{4}$$

where $h : \mathbb{R} \times \mathbb{R} \times [0,T] \to \mathbb{R}$ and $\bar{h} : \mathbb{R} \to \mathbb{R}$ is a final penalty term, which we want to minimize subject to the normal flow equation in (3).

More generally, let us consider the running-time cost functional

$$J(t_0,\phi,u) = \int_{t_0}^T L(\phi(\cdot,t),u(\cdot,t))\,dt + K(\phi),$$

with $t_0 \in [0,T]$ and the functionals $L : \mathcal{F} \times \mathcal{U} \to \mathbb{R}$ and $K : \mathcal{F} \to \mathbb{R}$, which, in the case of (4), are given by

$$L(\phi(\cdot,t),u(\cdot,t)) = \int_\Omega h(\phi(x,t),u(x,t),t)\,dx$$

and

$$K(\phi) = \int_\Omega \bar{h}(\phi(x,T))\,dx$$

with a little abuse of notation. Such functionals are assumed to be continuous in their arguments, i.e., ϕ and u for L as well as ϕ for K. Our goal is to find the control policy $u \in \mathcal{U}$ that minimizes $J(t,\phi,u)$ with (3) as a constraint. Thus, we define

$$V(\phi,t) = \inf_{u\in\mathcal{U}} J(t,\phi,u) \tag{5}$$

for $t \in [0,T]$.

Under mild conditions, the existence of viscosity solutions to (5) is shown ([24], Theorem 2, p. 905). Such a result is not constructive, but, by restricting the search to smooth solutions, the following holds.

Theorem 1. *Assume that there exists a continuously differentiable $\phi^\circ : \Omega \times [0,T] \to \mathbb{R}$ with $\phi^\circ(x,0) = \phi_0(x)$ and $V : \mathbb{R} \times [0,T] \to \mathbb{R}$ with $V(\cdot,T) = K(\cdot)$ such that*

$$V_t(\phi^\circ,t) - u^\circ\, V_\phi(\phi^\circ,t)\,|\nabla\phi^\circ| + L(\phi^\circ,u^\circ) = 0 \tag{6}$$

with

$$u^\circ \in \arg\min_{u\in\mathcal{U}} \left(L(\phi^\circ,u) - u\, V_\phi(\phi^\circ,t)\,|\nabla\phi^\circ|\right) \tag{7}$$

and $\phi_t^\circ + u^\circ\,|\nabla\phi^\circ| = 0$, where $V_\phi(\phi,t)$ is the Fréchet derivative of $V(\phi,t)$ with respect to ϕ and $V_t(\phi,t)$ is the partial time derivative of V. Then,

$$V(\phi^\circ,0) = \inf_{u\in\mathcal{U}:\phi_t+u\,|\nabla\phi|=0} J(0,\phi,u)\,. \tag{8}$$

Proof. The proof is in line with [29], Theorem 1, p. 6. In more detail, using

$$\dot{V}(\phi,t) = V_t + V_\phi\,\phi_t = V_t - u\,V_\phi\,|\nabla\phi|,$$

since $\phi_t + u\,|\nabla\phi| = 0$ and

$$\int_0^T \dot{V}(\phi(\cdot,t),t) + L(\phi(\cdot,t),u(\cdot,t))\,dt = V(\phi,T) - V(\phi,0) = K(\phi) - V(\phi,0) + \int_0^T L(\phi(\cdot,t),u(\cdot,t))\,dt$$

in general, from (6) and (7) we obtain

$$V(\phi,0) \le \int_0^T L(\phi(\cdot,t),u(\cdot,t))\,dt + K(\phi)$$

for all $u \in \mathcal{U}$, and hence (8) holds by choosing $\phi = \phi^\circ$. □

Let us focus on such a result by considering a simple example.

Example 1. *Consider a one-dimensional problem on the domain $\Omega \times [0,T]$ with $\Omega = [1,2]$ and $T = 2$. For the sake of simplicity, we search for an optimal control policy that depends only on time, i.e., $u : [0,T] \to \mathbb{R}$. Moreover, we focus on a quadratic cost*

$$L(\phi,u) = \int_\Omega (u(t))^2 dx = u^2\,,\; K(\phi) = \int_\Omega (\phi(x,T))^2 dx\,.$$

According to Theorem 1, a sufficient condition of optimality is given by

$$V_t + \min_u \left(u^2 - u\, V_\phi\, |\phi_x| \right) = 0$$

together with the related normal flow equation. Thus, we get

$$u^\circ = \frac{1}{2} V_\phi\, |\phi_x|$$

and

$$\begin{cases} V_t - \frac{1}{4} \left(V_\phi\, \phi_x \right)^2 = 0 \\ \phi_t + \frac{1}{2} V_\phi\, (\phi_x)^2 = 0\,. \end{cases} \tag{9}$$

If $\phi_0(x) = x$ and $K(\phi) = 1/3$, we can easily verify that the solution of (9) is given by $\phi(x,t) = x - t/2$ and $V(\phi,t) = \phi + t/4$.

The finite-horizon problem considered so far can be extended to an infinite horizon setting by dealing with discounted cost functionals such as

$$J_\infty(\phi, u) = \int_0^{+\infty} L(\phi(\cdot,t), u(\cdot,t)) \exp(-\lambda t)\, dt, \tag{10}$$

where $\lambda > 0$ and $L(\phi, u)$ is bounded for all $\phi \in \mathcal{F}, u \in \mathcal{U}$. The following result holds.

Theorem 2. *Assume that there exists a continuously differentiable $\phi^\circ : \Omega \times [0, +\infty] \to \mathbb{R}$ with $\phi^\circ(x,0) = \phi_0(x)$ and $V : \mathbb{R} \to \mathbb{R}$ such that*

$$-\lambda V(\phi^\circ) - u^\circ\, V_\phi(\phi^\circ)\, |\nabla \phi^\circ| + L(\phi^\circ, u^\circ) = 0, \tag{11}$$

with

$$u^\circ \in \arg\min_{u \in \mathcal{U}} \left(L(\phi^\circ, u) - u\, V_\phi(\phi^\circ)\, |\nabla \phi^\circ| \right) \tag{12}$$

and $\phi_t^\circ + u^\circ\, |\nabla \phi^\circ| = 0$, where $V_\phi(\phi)$ is the Fréchet derivative of $V(\phi)$ with respect to ϕ. Then,

$$V(\phi_0) = \inf_{\substack{u \in \mathcal{U}: \phi(\cdot,0) = \phi_0 \\ \phi_t + u\, |\nabla \phi| = 0}} \int_0^{+\infty} L(\phi(\cdot,t), u(\cdot,t)) \exp(-\lambda t)\, dt, \tag{13}$$

with $\lambda > 0$.

Proof. It is grounded on the theoretical framework reported in [2], which deals with the Hamilton-Jacobi-Bellman approach to the solution of infinite-horizon optimal control problems for systems described by ODEs. We will briefly sketch the demonstration by referring to [2] for details. Notice that

$$\begin{aligned} &\inf_u \left(\int_0^{+\infty} L(\phi(\cdot,t), u(\cdot,t)) \exp(-\lambda t)\, dt \right) = \\ &\inf_u \left(\int_0^{t} L(\phi(\cdot,s), u(\cdot,s)) \exp(-\lambda s)\, ds + \int_t^{+\infty} L(\phi(\cdot,s), u(\cdot,s)) \exp(-\lambda s)\, ds \right) \end{aligned}$$

for all $t \geq 0$ and, after a simple change of integration variable,

$$V(\phi_0) = \inf_u \left(\int_0^{t} L(\phi(\cdot,s), u(\cdot,s)) \exp(-\lambda s)\, ds + \exp(-\lambda t)\, V(\phi(\cdot,t)) \right).$$

Following ([2], Proposition 2.5, p. 102), according to the principle of dynamic programming, the function

$$t \mapsto k(t) := \int_0^t L(\phi(\cdot,s),u(\cdot,s)) \exp(-\lambda s)\, ds + \exp(-\lambda t)\, V(\phi(\cdot,t))$$

is optimal if and only if the pair (ϕ,u) is optimal, i.e., $(\phi,u) = (\phi^\circ,u^\circ)$. If we perturb the optimal solution in the interval $[t,t+dt]$, it follows an increase of $k(t)$, i.e., $k(t+dt) \geq k(t)$. Using $k(t+dt) = k(t) + k'(t)dt + o(dt)$ with $o(\cdot)$ denoting the remainder of order higher than one, we obtain $k'(t) \geq 0$ and, after computing the derivative of $k(t)$ and after multiplying for $\exp(\lambda t)$, we get (11) with (12) for (13) to hold. □

Remark 1. *After selecting the desired shape in Ω as the zero level set $\Gamma_0^{\text{ref}}(t)$ of a given reference function $\phi_{\text{ref}}(x,t)$, the goal is that of handling the zero level set $\Gamma_0(t)$ associated to the solution $\phi(x,t)$ to match $\Gamma_0^{\text{ref}}(t)$ as much as possible. Thus, a convenient choice of the cost functional to minimize is the symmetric difference between such level sets, i.e.,*

$$J = \int_0^T \eta\left(\Gamma_0(t)\,\Delta\,\Gamma_0^{\text{ref}}(t)\right) dt \tag{14}$$

where Δ stands for the symmetric difference operator, i.e., $\Gamma_0(t)\ \Delta\ \Gamma_0^{\text{ref}}(t) := (\Gamma_0(t) \cup \Gamma_0^{\text{ref}}(t)) \setminus (\Gamma_0(t) \cap \Gamma_0^{\text{ref}}(t))$, while η is an outer measure on $\mathbb{R}^q$ (see Figure 2). Though the proposed approach can deal with other performance indexes under the required assumptions (i.e., smoothness and, in the case of Theorem 2, the boundedness of $L(\cdot,\cdot)$), the choice of the cost strongly depends on the goal of matching the required shapes and thus it reduces to adopt a measure of the symmetric difference between level sets.

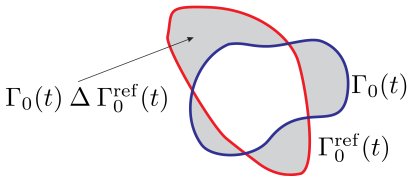

Figure 2. Area (in grey) of the symmetric difference between two level sets (in blue and red).

Unfortunately, it is difficult to find an expression for the minimizer in (7) or (12) (especially when we search for control laws that depend on both space and time) and obtain the exact analytic solution of (6) or (11) in general. Thus, numerical methods are well-suited to finding approximate solutions, as shown in the next section, where we deal with two case studies.

3. Numerical Results

In this section, we present the simulation results obtained in solving optimal control problems concerning the tracking of reference curves both in two and three dimensions (2D and 3D, for short). Specifically, we will search for a mapping $(x,t) \mapsto u(x,t)$ that drives the zero level set $\Gamma_0(t)$ of the solution $\phi(x,t)$ of (3) in order to match the zero level set $\Gamma_0^{\text{ref}}(t)$ of the function $\phi_{\text{ref}}(x,t)$ by using the cost functional

$$J = \int_0^T \int_\Omega \left(\hat{H}_\tau(\phi(x,t)) - \hat{H}_\tau(\phi_{\text{ref}}(x,t))\right)^2 dx\, dt, \tag{15}$$

with $\hat{H}_\tau$ denoting the approximate Heaviside step function, i.e.,

$$\hat{H}_\tau(\xi) := \frac{1}{2} + \frac{1}{2}\tanh\left(\frac{\xi}{\tau}\right),$$

where $\tau > 0$ modulates the smoothness of the approximation.

The solution of (6) with (7) was found by the approach presented in [27] (see also [30]), where the minimization in (7) was obtained by using the *fmincon* routine of the Matlab Optimization Toolbox.

We refer to such a solution procedure as Guo-Sun numerical optimization (GSNO) method. For the purpose of comparison, we considered also the approach presented in [24], where the extended Ritz method is adopted to find parametrized approximate solutions by using a Gauss-Newton descent method. Such a method is treated by using a computationally efficient algorithm based on the extended Kalman filter (see [24] for details), thus it will be briefly referred to as EKF-based optimization (EKFO).

We considered two case studies in 2D and 3D. As regards the 2D example, we focused on a space domain $\Omega = [-0.75, +0.75] \times [-0.5, +0.5]$, discretized using a regular grid of 75×50 points for the numerical solution of (3). The time interval was fixed to $[0, 1.5]$. The sampling time Δt was chosen equal to 0.03, i.e., the simulation was completed after 50 time steps. Concerning the 3D case, we adopted a domain $\Omega = [-1.5, 1.5] \times [-1.0, 1.0] \times [-1.0, 1.0]$ sampled with a grid made of $90 \times 60 \times 60$ nodes. The time interval for the simulation was $[0, 1.5]$ using a time step $\Delta t = 0.05$, i.e., the simulation was performed in 30 time steps. In both case studies, we fixed τ to 10^{-2} in (15).

Concerning the EKFO, we chose one-hidden-layer feedforward neural networks with sigmoidal activation functions as parameterized approximating functions. In particular, we tested various numbers of basis functions, i.e., we considered $n = 5$, 10, and 15 neurons. Such numbers ensured sufficient accuracy with quite simple approximating structures. All the results were averaged on 50 randomly-chosen initial weights. Similarly, we randomly generated the initial points of the *fmincon* routine of the GSNO. We used a personal computer with a 2.6 GHz Intel Xeon CPU with 64 GB of RAM running Windows 10 to perform the simulations.

Figures 3 and 4 show the results gained by using the GSNO with the reference and simulated fronts at different time instants. Table 1 reports the means of the optimal cost J° and of the computational time $\overline{T}$ required to perform the computations with the GSNO and EKFO over 50 trials. Figure 5 displays the boxplots of the cost J° and of the computational time $\overline{T}$ obtained with 10 neurons. As compared with the EKFO, the GSNO is computationally much less demanding, especially in the 3D case study. In terms of resulting optimal cost, the results given by EKFO and GSNO are quite close.

Table 1. Summary of the means of optimal costs and optimization times over 50 simulation runs for the GSNO and EKFO.

	Mean of J°			**Mean of $\overline{T}$ (s)**		
	GSNO	**EKFO**	***n***	**GSNO**	**EKFO**	***n***
2D	1.24×10^{-3}	1.19×10^{-4}	5	3.18×10^{2}	3.46×10^{2}	5
		1.38×10^{-4}	10		5.19×10^{2}	10
		3.77×10^{-4}	15		8.41×10^{2}	15
3D	8.57×10^{-4}	5.87×10^{-4}	5	6.08×10^{3}	1.39×10^{4}	5
		4.52×10^{-4}	10		2.82×10^{4}	10
		1.27×10^{-4}	15		7.04×10^{4}	15

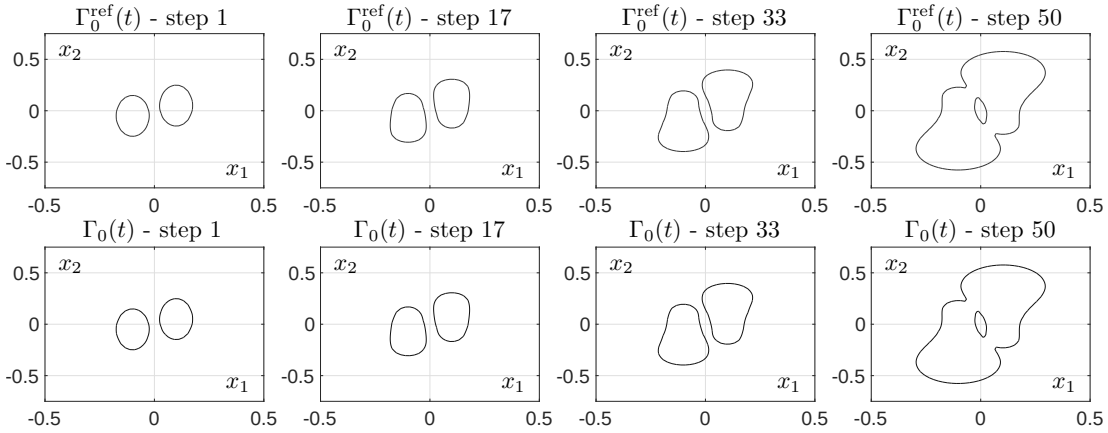

Figure 3. 2D front tracking snapshots obtained with the GSNO.

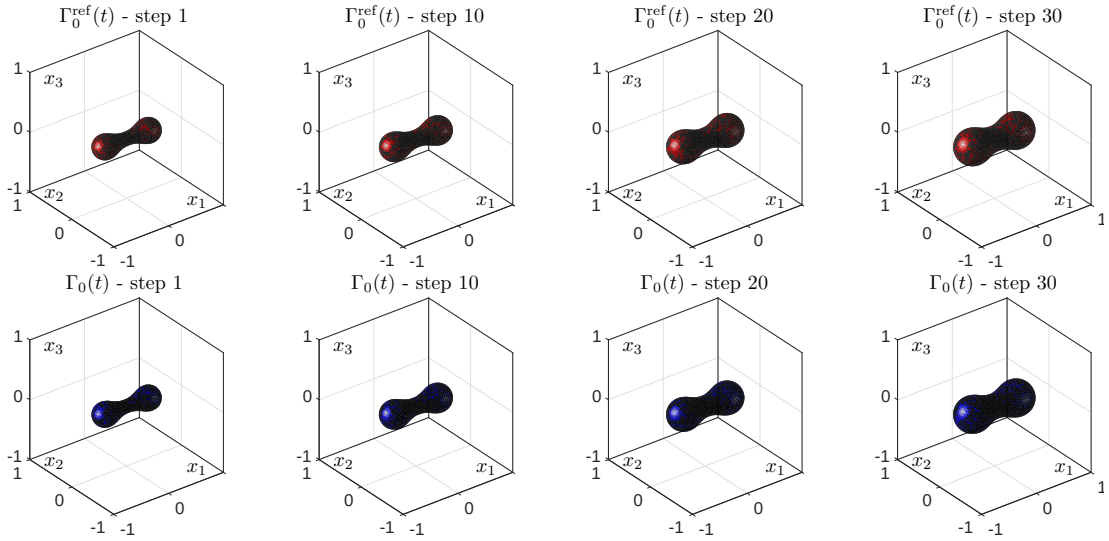

Figure 4. 3D front tracking snapshots obtained with the GSNO.

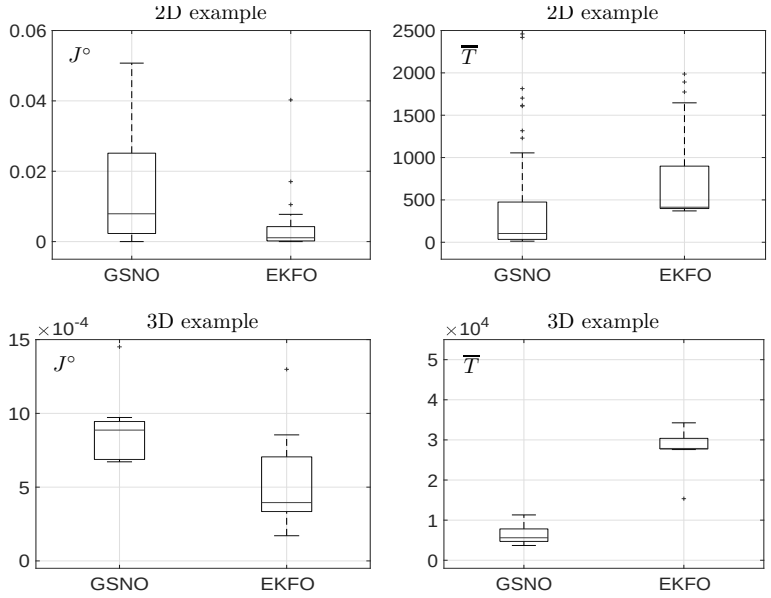

Figure 5. Performance comparison between the GSNO and EKFO (with $n = 10$ basis functions): the boxplots of optimal cost and optimization time over a batch of 50 simulations show the "average" behavior of such indexes over all the simulation runs.

4. Conclusions

We have addressed the problem of constructing propagating fronts by formulating optimal control problems with a front dynamics described by Hamilton-Jacobi equations such as the normal flow equations. Numerical solutions of such problems have been shown in two case studies and compared with previously-developed approaches. The results are quite satisfying and suggest the extension of the proposed approach to other kinds of Hamilton-Jacobi equations for front modeling such as the mean curvature flow equation. Another direction of research is the investigation of suitable stability conditions when dealing with infinite-horizon problems and the combination of level set methods with other complex phenomena in fluid dynamics such those described by Navier-Stokes equations [31].

Author Contributions: Conceptualization, A.A., P.B., M.G.; methodology, A.A., P.B., M.G.; software, P.B., M.G.; validation, R.C.; formal analysis, R.C.; investigation, A.A., P.B., M.G.; resources, M.G.; data curation, M.G.; writing—original draft preparation, P.B., M.G.; writing—review and editing, A.A., P.B., M.G.; visualization, P.B.; supervision, R.C.; project administration, A.A.; funding acquisition, A.A.

Funding: This research was funded by AFOSR with grant FA9550-15-1-0530.

Acknowledgments: The authors are indebted to the Air Force Office of Scientific Research for financial support.

Conflicts of Interest: The authors declare no conflict of interest.

Abbreviations

The following abbreviations are used in this manuscript:

EKF	extended Kalman filter
EKFO	EKF optimization
GSNO	Guo-Sun numerical optimization
ODE	ordinary differential equation
PDE	partial differential equation

References

1. Osher, S.; Sethian, J. Fronts propagating with curvature-dependent speed: Algorithms based on Hamilton-Jacobi formulations. *J. Comput. Phys.* **1988**, *79*, 12–49. [CrossRef]
2. Bardi, M.; Capuzzo-Dolcetta, I. *Optimal Control and Viscosity Solutions of Hamilton Jacobi Bellmann Equations*; System & Control: Foundations & Applications, Birkäuser: Boston, MA, USA; Basel, Switzerland; Berlin, Germany, 1997.
3. Otieno, G.; Koske, J.K.; Mutiso, J.M. Cost effectiveness analysis of optimal malaria control strategies in Kenya. *Mathematics* **2016**, *4*, 14. [CrossRef]
4. El Kihal, F.; Abouelkheir, I.; Rachik, M.; Elmouki, I. Role of media and effects of infodemics and escapes in the spatial spread of epidemics: A stochastic multi-region model with optimal control approach. *Mathematics* **2019**, *7*, 304. [CrossRef]
5. Abouelkheir, I.; El Kihal, F.; Rachik, M.; Elmouki, I. Optimal impulse vaccination approach for an SIR control model with short-term immunity. *Mathematics* **2019**, *7*, 420. [CrossRef]
6. Beard, R.W.; Saridis, G.N.; Wen, J.T. Approximate solutions to the time-invariant Hamilton–Jacobi–Bellman equation. *J. Optim. Theory Appl.* **1998**, *96*, 589–626. [CrossRef]
7. Alessandri, A.; Gaggero, M.; Zoppoli, R. Feedback optimal control of distributed parameter systems by using finite-dimensional approximation schemes. *IEEE Trans. Neural Netw. Learn. Syst.* **2012**, *23*, 984–996. [PubMed]
8. Sana, M.; Mustahsan, M. Finite element approximation of optimal control problem with weighted extended B-splines. *Mathematics* **2019**, *7*, 452. [CrossRef]
9. Sethian, J. *Level Set Methods and Fast Marching Methods*, 2nd ed.; Cambridge University Press: Cambridge, UK, 1999; Volume 3.
10. Sethian, J.; Smereka, P. Level set methods for fluid interfaces. *Annu. Rev. Fluid Mech.* **2003**, *35*, 341–372. [CrossRef]
11. Osher, S.; Fedkiw, R. *Level Set Methods and Dynamic Implicit Surfaces*; Volume 153: Applied Mathematical Sciences; Springer-Verlag: New York, NY, USA, 2003.
12. Kimmel, R. *Numerical Geometry of Images*; Springer-Verlag: New York, NY, USA, 2004.
13. Bronsard, L.; Wetton, B. A numerical method for tracking curve networks moving with curvature motion. *J. Comput. Phys.* **1995**, *120*, 66–87. [CrossRef]
14. Kim, Y.; Lai, M.C.; Peskin, C. Numerical simulations of two-dimensional foam by the immersed boundary method. *J. Comput. Phys.* **2010**, *229*, 5194–5207. [CrossRef]
15. Fursikov, A. *Optimal Control of Distributed Systems*; AMS: Providence, RI, USA, 2000.
16. Baranovskii, E. Solvability of the stationary optimal control problem for motion equations of second grade fluids. *Sib. Electron. Math. Rep.* **2012**, *9*, 554–560.
17. Baranovskii, E. Optimal control for steady flows of the Jeffreys fluids with slip boundary condition. *J. Appl. Ind. Math.* **2014**, *8*, 168–176. [CrossRef]
18. Plekhanova, M. Nonlinear Degenerate Fractional Order Evolution Equations. Solvability of Optimal Control Problems. Ph.D. Thesis, Chelyabinsk State University, Chelyabinsk, Russia, 2017.

19. Hinze, M.; Ziegenbalg, S. Optimal control of the free boundary in a two-phase Stefan problem. *J. Comput. Phys.* **2007**, *223*, 657–684. [CrossRef]
20. Bernauer, M.; Herzog, R. Optimal control of the classical two-phase Stefan problem in level set formulation. *SIAM J. Sci. Comput.* **2011**, *33*, 342–363. [CrossRef]
21. Haque, M.; Rahmani, A.; Egerstedt, M.; Yezzi, A. Efficient foraging strategies in multi-agent systems through curve evolutions. *IEEE Trans. Autom. Control* **2014**, *59*, 1036–1041. [CrossRef]
22. Alessandri, A.; Bagnerini, P.; Gaggero, M. Optimal control of level sets dynamics. In Proceedings of the 2014 American Control Conference, Portland, OR, USA, 4–6 June 2014; pp. 2208–2213.
23. Alessandri, A.; Bagnerini, P.; Cianci, R.; Gaggero, M. Optimal control of level sets generated by the normal flow equation. In *Theory, Numerics and Applications of Hyperbolic Problems I*; Klingenberg, C., Westdickenberg, M., Eds.; Springer International Publishing: Cham, Switzerland, 2018; Volume 236, pp. 29–41.
24. Alessandri, A.; Bagnerini, P.; Gaggero, M. Optimal control of propagating fronts by using level set methods and neural approximations. *IEEE Trans. Neural Netw. Learn. Syst.* **2019**, *30*, 902–912. [CrossRef] [PubMed]
25. Zoppoli, R.; Sanguineti, M.; Parisini, T. Approximating networks and extended Ritz method for the solution of functional optimization problems. *J. Optim. Theory Appl.* **2002**, *112*, 403–440. [CrossRef]
26. Cambronero, J.; Álvarez, J. Systems of Hamilton-Jacobi equations. *J. Nonlinear Math. Phys.* **2019**, *26*, 650–658. [CrossRef]
27. Guo, B.Z.; Sun, B. Numerical solution to the optimal birth feedback control of a population dynamics: Viscosity solution approach. *Optim. Control Appl. Methods* **2005**, *26*, 229–254. [CrossRef]
28. Alessandri, A.; Bagnerini, P.; Gaggero, M. Extended Kalman filtering to design optimal controllers of fronts generated by level set methods. In Proceedings of the 2016 IEEE 55th Conference on Decision and Control (CDC), Las Vegas, NV, USA, 12–14 December 2016; pp. 3966–3971.
29. Ekeland, I.; Turnbull, T. *Infinite-Dimensional Optimization and Convexity*; Chicago Lectures in Mathematics; The University of Chicago Press: Chicago, IL, USA, 1983.
30. Guo, B.Z.; Sun, B. A new algorithm for finding numerical solutions of optimal feedback control. *IMA J. Math. Control Inf.* **2009**, *26*, 95–104. [CrossRef]
31. Alessandri, A.; Bagnerini, P.; Gaggero, M.; Mantelli, L.; Santamaria, V.; Traverso, A. Black-box modeling and optimal control of a two-phase flow by using Navier-Stokes equations and level set methods. In Proceedings of the 2018 Annual American Control Conference (ACC), Milwaukee, WI, USA, 27–29 June 2018; pp. 3429–3434.